

THEORETICAL AND EXPERIMENTAL INVESTIGATION OF THE EVACUATED TUBE SOLAR WATER HEATER SYSTEM

by

Phrut SAKULCHANGSATJATAI*, **Chaiwat WANNAGOSIT**,
Niti KAMMUANG-LUE, and **Pradit TERDTON**

Department of Mechanical Engineering, Faculty of Engineering,
Chiang Mai University, Chiang Mai, Thailand

Original scientific paper
<https://doi.org/10.2298/TSCI180128002S>

In this study, the evacuated tube solar water heater system using thermosyphon has been investigated experimentally as well as theoretically. Solar radiation and ambient temperature data from Chiang Mai province were used for the modelling system by explicit finite difference method. The effects of thermosyphon diameters and number of evacuated tubes on the net saving of solar water heater system were analyzed. The mathematical results showed that the optimal number of evacuated tubes and thermosyphon diameter occurs at eight evacuated tubes, which are 15.88 mm of evaporator diameter and 22.22 mm of condenser diameter under personal hygiene conditions. The solar water heater system at optimal parameters was constructed and tested for the system prototype. The theoretical results were validated by the experimental results. It was found that the theoretical results can be used to predict temperature, heat transfer rate, and thermal efficiency to show good agreement with the experimental results as well as previous research. The experimental and theoretical results showed that the maximum temperature for hot water was 65.25 °C and 71.66 °C, respectively. Moreover, the thermal efficiency of the system based on the theoretical result was 60.11%, with relative error being about 3.04% of the experimental result.

Key words: *solar water heater system, two-phase closed thermosyphon, explicit finite difference method, evacuated tube collector*

Introduction

Solar energy is one form of renewable energy that can be used for long-term periods. It is also environmentally friendly. One technological tool for solar energy utilization is the solar water heater. Solar energy is absorbed in thermal form and concurrently transferred into hot water by a solar collector. Presently, the collectors used in solar systems comprise several types such as flat plate collector, evacuated tube collector and heat pipe collector [1]. The evacuated tube solar collector has shown better performance than the flat plate solar collectors, particularly for high temperature operation [2]. This is because of the high-absorption capability of the selective surface coating and vacuum insulation of the absorber surface. Evacuated tube solar collectors can be classified into three types, namely:

- water-in-glass evacuated tube collector [3-5],
- single-phase thermosyphon evacuated tube collector [3, 5], and
- two-phase closed thermosyphon evacuated tube collector [5-7].

* Corresponding author, e-mail: phrut@eng.cmu.ac.th

Evacuated tube solar collectors have been continually developed, such as using the two-phase closed thermosyphon in the evacuated tube collector [6-10]. It is also equipment with a very high thermal conductivity used for heat transfer [11]. From previous research concerning the thermosyphon, it is apparent that the filling ratio [8], working fluid [9], and diameters of the thermosyphon [10] influence the performance of the solar collector.

As previously mentioned, many researchers have been focused on performance improvement using the experimental method and theoretical method in order to develop the thermosyphon for a solar water heater system. Thus, the thermosyphon design is very important for the solar water heater system because it is used as equipment for heat transfer from the evacuated tube collector to the water. The factors of thermosyphon design include the diameter of the thermosyphon [10] and the ratio of evaporator length to condenser length [12]. Accordingly, theoretical studies have been performed for the prediction of thermosyphon and solar water system design. At the same time, the thermosyphon has also been studied and calculated by thermal resistance method [2, 5, 12]. Azad [12] studied the theoretical and experimental design of a flat plate solar collector utilizing heat pipes. The results showed that the heat pipes possessed good concurrence between the measured and theoretical results, in which the error was 5.3% of the experimental results. Furthermore, the model can help predict the optimum ratio for the thermosyphon tube for configurations in the experimental work. In the next period, transient system simulation (TRNSYS) is used for studying the solar water heater system [3-5, 13]. Budihardjo and Morrison [4] and Morrison *et al.* [3] studied the water-in-glass evacuated tube solar water heater (ETSWH) in comparison the flat-plate with boost tank. It was found that the annual energy savings from the water-in-glass evacuated tube collector was lower than for the flat-plate collector about 6.1% at lower temperature. Chow *et al.* [5] studied the experimental and numerical models for two types of evacuated tube collectors. Both *open* and *closed* thermosyphon types were set up under the same conditions. The results showed that the heat of the two-phase type was higher than the single-phase type by 12.9%.

As in the previous studies mentioned previously, the TRNSYS program is used for the solar water heater design to evaluate and design the solar water heater for a single-phase thermosyphon. On the other hand, it can be seen that the two-phase closed thermosyphon is studied by thermal resistance method for application with a flat-plate collector. It can be said that the application of the two-phase closed thermosyphon with the evacuated tube collector is rather interesting to study, mainly because many parameters have affected the design and operation of the ETSWH with the two-phase closed thermosyphon. It should be noted that sufficient information is needed to create optimal designs for the thermosyphon and the ETSWH system configuration.

In this study, the mathematical model for evacuated tube solar hot water using a thermosyphon system was calculated using the explicit finite difference method (EFDM). The effects of thermosyphon diameter and number of evacuated tubes on the heat transfer rate were studied. The water heat rate was converted to electrical price for determining the optimal design by thermoeconomic analysis. These effects of parameters were used to design and construct the solar water heater system for experimental trials. The accuracy of the mathematical model results, temperatures, heat rate of water and thermal efficiency were investigated using the experimental results under the same operating conditions.

System description

The solar water heater system consists of a water storage tank, evacuated tube, and thermosyphon, as shown in fig. 1. The collector fin and thermosyphon were attached in the

clearance between the inner evacuated tube walls of the double-layer tube, as shown in the cross-sectional view of fig. 1(b). Firstly, solar radiation was transmitted through the outer part of the evacuated tube wall and incident on the inner surface of the evacuated tube collector. Solar radiation was absorbed by the absorber surface of the inner evacuated tube wall. The heat increased in absorber surface and then transferred to the evaporator section by collector fin. The working fluid in the thermosyphon was evaporated and flowed to the condenser section, which was held in the manifold. In the meantime, the water in a storage tank was pumped to the manifold and flowed out through to the condenser section. Heat in the condenser section was transferred to the water by convective heat transfer of water flow through the condenser surface. The working fluid of the thermosyphon was condensed by latent heat of vapor and water temperature increasing at the same time.

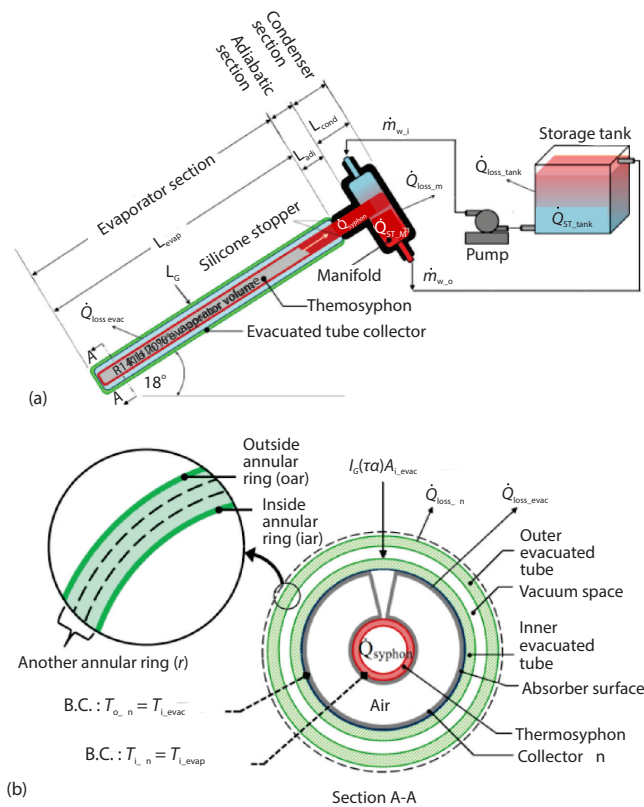


Figure 1. Schematic diagram and cross-sectional view of evacuated tube solar water heater system; (a) schematic diagram of solar water heater system, (b) cross-sectional views of the evacuated tube

The specifications are shown in tab. 1, which are used for the control parameters of the mathematical model of the ETSWH system.

Table 1. The specification of the evacuated tube solar water heater system

Data	Details	Units	Data	Details	Units
Evacuated tube			Thermosyphon		–
Length, L_{evac}	1800	[mm]	Material	L-Type copper	–
Outer tube diameter, D_{o_evac}	58	[mm]	Evaporator length, L_{evap}	1700	[mm]
Inner tube diameter, D_{i_evac}	47	[mm]	Adiabatic length, L_{adi}	50	[mm]
Absorptance, α	0.92	–	Condenser length, L_{cond}	80	[mm]
Transmittance, τ	0.907	–	Working fluid, type	R141b	–
Emittance, ε	0.08	–	Working fluid volume	70% of V_{evap}	–
Collector fin		–	Water flow rate, \dot{m}	0.03 [11]	[kgs ⁻¹]
	Aluminum	–	Water storage tank	100	[L]

Mathematical model and method

Mathematical model

From the previous section, simulating the solar water heater system should involve setting the system description for the control parameters, assumptions and boundary conditions applied for the components of the solar water heater system. The mathematical model was calculated for the temperature of each component, water heat rate and thermal efficiency. However, assumptions and boundary conditions are defined to simplify the simulation of the ETSWH system. The assumptions in this study were:

- Solar radiation is considered on the half surface of the evacuated tube collector, but radiation loss is considered in all directions around the tube.
- Heat transfers of the thermosyphons and the heat loss of evacuated tubes and collector fins are identical.
- Heat loss at the adiabatic section is negligible due to consideration of the adiabatic process.
- Internal resistances of thermosyphon (Z_4 , Z_5 , and Z_6) are usually neglected due to their relatively small magnitude.
- Solar radiation and ambient air temperature in Chiang Mai, Thailand were used.

To consider the boundary conditions in this study, each of the components was divided into annual rings, which consist of an outside annual ring (*oar*), inside annual ring (*iar*), and other annual rings (*r*). A sample of the annual ring is shown in fig. 1(b). Consequently, the boundary conditions in this study were: the temperature at the outside annual ring for each of the domains is equal to the temperature at the inside annual ring for the next domain, as shown in fig. 1(b).

The EFDM [14] approach and MATLAB program were employed to simulate the ETSWH system based on Thailand's climatic data in Chiang Mai province. The conservation of energy was applied to the components in r - θ - z direction. The governing equation was:

$$\frac{1}{\alpha} \frac{\partial T}{\partial t} = \frac{\partial^2 T}{\partial r^2} + \frac{1}{r} \frac{\partial T}{\partial r} + \frac{1}{r^2} \frac{\partial^2 T}{\partial \theta^2} + \frac{\partial^2 T}{z^2} + \frac{\dot{q}}{k} \quad (1)$$

From the assumptions, the boundary conditions and the EFDM are applied to the components of the mathematical model.

Evacuated tube domain

Solar radiation transmitted through the outer evacuated tube wall and was subsequently absorbed by the absorber surface, as shown in fig. 1(b). Applying energy balance on the control surface of the evacuated tube:

$$\dot{Q}_{ST_evac} = I_G (\tau\alpha) A_{i_evac} - \dot{Q}_{loss_evac} \quad (2)$$

where \dot{Q}_{ST_evac} [W] is the remainder of thermal energy stored on the absorber surface, I_G [Wm^{-2}] – the solar radiation incident on the surface of evacuated tubes, and \dot{Q}_{loss_evac} [W] – the heat loss of evacuated tubes to surrounding, which can be calculated by the convection heat transfer from Nusselt number according to Churchill and Bernstein correlation equation [15]:

$$Nu_d = \frac{h_{air} D_{o_evac}}{k_{o_evac}} = 0.3 + \frac{0.62 Re_d^{1/2} Pr_{air}^{1/3}}{\left[1 + \left(\frac{0.4}{Pr_{air}}\right)^{2/3}\right]^{1/4}} \left[1 + \left(\frac{Re_d}{282000}\right)^{5/8}\right]^{4/5} \quad (3)$$

where Pr is the Prandtl number of air and Re_d is the Reynolds number. The Reynolds number can be calculated from the air property, wind velocity and diameter of the outer evacuated tube, D_{o_evac} .

The thermal energy stored in the absorber surface was obtained from eq. (2). Therefore, the outside annual ring temperature of inner evacuated tube, $T_{i_evac(oar, \theta, z)}^n$, can be calculated by modifying the radiation heat transfer in two-surface enclosures:

$$T_{i_evac(oar, \theta, z)}^n = \sqrt[4]{\frac{(\dot{Q}_{ST_evac}) \left[\frac{1}{\epsilon_{i_evac}} + \frac{r_{i_evac}}{r_{o_evac}} \left(\frac{1 - \epsilon_{o_evac}}{\epsilon_{o_evac}} \right) \right]}{\sigma A_{i_evac}}} + [T_{o_evac(oar, \theta, z)}^n]^4} \quad (4)$$

In addition, another annual ring temperature was applied from the EFDM in eq. (1):

$$T_{evac(r, \theta, z)}^n = \alpha \Delta t \left(\frac{\partial^2 T}{\partial r^2} + \frac{1}{r} \frac{\partial T}{\partial r} + \frac{1}{r^2} \frac{\partial^2 T}{\partial \theta^2} + \frac{\partial^2 T}{z^2} \right) + T_{evac(r, \theta, z)}^{n-1} \quad (5)$$

The inside annual ring temperature of the inner evacuated tube, $T_{i_evac(iar, \theta, z)}^n$, was obtained from this section and was defined as equal to the outside annual ring temperature of the outer collector fin, $T_{o_fin(oar, \theta, z)}^n$, following the boundary conditions. The collector of fin temperature was calculated in the next section.

Collector fin domain

The collector fin was inserted into the clearance between the inner evacuated tube walls, as shown in fig. 1(b). The heat accumulated at the absorber surface was transferred to the collector fin. The heat transfer of the collector fin was divided into two parts: accumulated heat at the collector fin surface and heat loss to the inside air of the evacuated tube by convection heat transfer. The inside air temperature of the evacuated tube, T_{air_evac} , increases by increasing the collector fin surface temperature. The convection heat transfers from the collector fin to the inside air of the evacuated tube, \dot{q}_{loss_fin} :

$$\dot{q}_{loss_fin} = h_{i_evac} (T_{o_fin(iar, \theta, z)}^n - T_{air_i_evac}^{n-1}) \quad (6)$$

where h_{i_evac} [$Wm^{-2}K^{-1}$] is the natural-convection heat transfer coefficient [15] at the inner evacuated tube.

Therefore, the temperature at the present time of an inside annual ring at the outer collector fin can be modified from eq. (1):

$$T_{o_fin(iar, \theta, z)}^n = \alpha \Delta t \left(\frac{\partial^2 T}{\partial r^2} + \frac{1}{r} \frac{\partial T}{\partial r} + \frac{1}{r^2} \frac{\partial^2 T}{\partial \theta^2} + \frac{\partial^2 T}{z^2} - \frac{\dot{q}_{loss_fin}}{k_{fin}} \right) + T_{o_fin(iar, \theta, z)}^{n-1} \quad (7)$$

In addition, another annual ring temperature of the outer collector fin at the present time can be calculated by applying eq. (1), which is the same as eq. (5).

As seen in fig. 1(b), the collector fin was made of aluminum, which has high thermal conductivity. In this work, it can be assumed that the temperature outside the inner collector fin was equal to the inside of the outer collector fin due to the high thermal conductivity of aluminum. Thus, the inside air temperature at the present time can be calculated:

$$T_{air_i_evac}^n = \frac{\dot{q}_{loss_fin} A_{o_fin} (\Delta t)}{M_{air_i_evac} C_p} + T_{air_i_evac}^{n-1} \quad (8)$$

From eq. (6) to eq. (8), the temperatures of outer and inner collector fin were obtained. After that, the temperatures of the collector fin were defined as equal to the boundary conditions of thermosyphon and used to calculate the thermosyphon domain.

Thermosyphon domain

The thermosyphon domain was divided into three parts comprising the evaporator section, the adiabatic section and the condenser section, as presented in fig 1. Following the boundary conditions defined previously, the evaporator temperature was modified from eq. (1):

$$T_{\text{evap}(r,\theta,z)}^n = \alpha \Delta t \left(\frac{\partial^2 T}{\partial r^2} + \frac{1}{r} \frac{\partial T}{\partial r} + \frac{1}{r^2} \frac{\partial^2 T}{\partial \theta^2} + \frac{\partial^2 T}{z^2} \right) + T_{\text{evap}(r,\theta,z)}^{n-1} \quad (9)$$

The inside annual ring of the evaporator section, $T_{\text{evap(iar, } \theta, z)}^n$, was used for calculating the inside annual ring of the condenser section, $T_{\text{cond(iar, } \theta, z)}^n$, from the thermal resistance:

$$T_{\text{cond(iar, } \theta, z)}^n = T_{\text{evap(iar, } \theta, z)}^n - \left[\dot{Q}_{\text{syphon}} (Z_3 + Z_7) \right] \quad (10)$$

where Z_3 and Z_7 are the thermal resistance of film boiling and film condensation, respectively [16], which can be calculated:

$$Z_3 = Z_{3p} F + Z_{3f} (1 - F) \quad (11)$$

$$Z_{3f} = \frac{CQ^{1/3}}{D_i^{4/3} g^{1/3} L_e \Phi_2^{4/3}} \quad (12)$$

$$Z_{3p} = \frac{1}{\Phi_3 g^{0.2} Q^{0.4} (\pi D_{in} L_e)^{0.6}} \quad (13)$$

if $Z_{3p} < Z_{3f}$ define $Z_3 = Z_{3p}$

$$Z_7 = \frac{CQ^{1/3}}{D_{in}^{4/3} g^{1/3} h(\Phi_2)^{4/3}} \quad (14)$$

where $Re_f > 1300$ can be calculated from $Re_f = 4Q/h\mu\pi D_i$

$$Z_7 = \frac{CQ^{1/3}}{D_{in}^{4/3} g^{1/3} h_{fg}(\Phi_2)^{4/3}} \times 191 Re_f^{-0.733} \quad (15)$$

where C is $(1/4)(3/\pi)^{4/3} = 0.235$, Φ_2 and Φ_3 can be calculated

$$\Phi_2 = \left(\frac{h_{fg} k_f^3 \rho_f^2}{\mu_f} \right)^{0.25} \quad (16)$$

$$\Phi_3 = 0.32 \frac{\rho_f^{0.65} k_f^{0.3} c_{pf}^{0.7}}{\rho_v^{0.25} h_{fg}^{0.4} \mu_f^{0.1}} \left[\frac{P_v}{P_a} \right]^{-0.23} \quad (17)$$

In addition, \dot{Q}_{syphon} is the remainder of thermal energy in the thermosyphon:

$$\dot{Q}_{\text{syphon}} = I_G A_{\text{evac}} (\tau \alpha) - \dot{Q}_{\text{loss_evac}} - \dot{q}_{\text{loss_fin}} A_{\text{o_fin}} \quad (18)$$

The inside annual ring temperature of the condenser section was obtained from eq. (10). Therefore, another annual ring temperature of condenser section, $T_{\text{cond}(r, \theta, z)}^n$, was modified from eq. (1), which was the same as eq. (9) for the evaporator section. The outside annual

ring of the condenser section, $T_{\text{cond(oar, } \theta, z)}^n$, was obtained in this section, which was used to calculate the convection heat transfer of the condenser and water circulation in the manifold.

Manifold domain

Heat accumulation in the condenser was transferred to water circulate in the manifold by the convective heat transfer. The water heat rate, \dot{Q}_{ST_m} :

$$\dot{Q}_{\text{ST}_m} = \frac{M_{w_m} c_p (T_{w_m}^n - T_{w_m}^{n-1})}{\Delta t} \quad (19)$$

From the energy balance on the manifold, the water temperature within the manifold:

$$T_{w_m}^n = \frac{(\dot{Q}_{\text{convect}_m} + \dot{Q}_{\text{wi}} - \dot{Q}_{\text{wo}} - \dot{Q}_{\text{loss}_m}) \Delta t}{M_{w_m} c_p} + T_{w_m}^{n-1} \quad (20)$$

where M_{w_m} [kg] is the mass of water in the manifold, Δt [s] – the storage time interval, \dot{Q}_{loss_m} – the natural-convection heat transfer and $\dot{Q}_{\text{convect}_m}$ is the heat convection of water as calculated from the thermal resistance between water and the external surface of condenser section, Z_{convect_m} , which can be expressed:

$$\dot{Q}_{\text{convect}_m} = \frac{T_{\text{cond(oar, } \theta, z)}^n - T_{w_m}^{n-1}}{Z_{\text{convect}_m}} \quad (21)$$

where Z_{convect_m} [KW^{-1}] is determined from the water flow rate using a flow cross cylinder. The $\dot{Q}_{\text{convect}_m}$ in eq. (14) should be compared with \dot{Q}_{siphon} in eq. (18) to simplify the simulation of the ETSWH system and is selected by the minimum heat rate.

Storage tank domain

Heat accumulation in water at the storage tank, $\dot{Q}_{\text{ST}_\text{tank}}$, can be defined:

$$\dot{Q}_{\text{ST}_\text{tank}} = \frac{M_{w_tank} c_p (T_{w_tank}^n - T_{w_tank}^{n-1})}{\Delta t} \quad (22)$$

From the energy balance on the storage tank, energy balance on a control volume was applied and converted to calculate water temperature within the storage tank:

$$T_{w_tank}^n = \left[\frac{(\dot{Q}_{\text{i}_\text{tank}} - \dot{Q}_{\text{o}_\text{tank}} - \dot{Q}_{\text{loss}_\text{tank}}) \Delta t}{M_{w_tank} c_p} \right] + T_{w_tank}^{n-1} \quad (23)$$

From eq. (23), the heat loss of the storage tank to the surroundings, $\dot{Q}_{\text{loss}_\text{tank}}$, can be calculated by the temperature difference of the water within the storage tank and ambient divide thermal resistance of the storage tank, $Z_{\text{loss}_\text{tank}}$. The thermal resistance of the storage tank can be calculated:

$$Z_{\text{loss}_\text{tank}} = \left(\frac{t_{\text{tank}}}{A_{\text{tank}} k_{\text{tank}}} \right) + \left(\frac{t_{\text{ins}}}{A_{\text{ins}} k_{\text{ins}}} \right) + \left(\frac{1}{h_{\text{air}} A_{\text{ins}}} \right) \quad (24)$$

where t_{tank} [m] is the wall thickness of the storage tank, t_{ins} [m] – the insulator thickness, A_{tank} and A_{ins} [m^2] are area of the water storage tank and area of the insulated, k_{tank} and k_{ins} [$\text{Wm}^{-1}\text{K}^{-1}$] – the thermal conductivity, respectively.

The water heat rate of the storage tank was calculated from eq. (24), which was used to calculate the thermal efficiency of the ETSWH [15]:

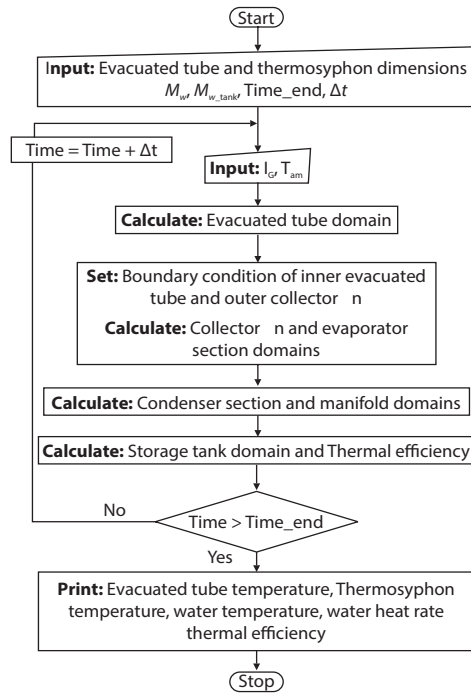


Figure 2. Computational steps the models

$$\eta_{\text{system}} = \frac{\dot{Q}_{\text{ST_tank}}}{I_G(\tau\alpha)A_{i_evac}} \quad (25)$$

The writing step for calculation can be presented in the flow chart for modelling of the solar water heater system, as shown in fig. 2. Appropriate annular rings for each component were analyzed by short calculation time required and nearly constant standard deviation criteria. Thus, these results show that the annular rings of all components were divided into four annual rings consisting of 7860 elements. In addition, the time step, Δt , in the mathematical model employed 1 minute, while the circumferential step, $\Delta\theta$, was divided into 15° intervals. The longitudinal step, Δz , was divided into two parts as the evacuated tube, the evaporator section, the adiabatic section, and collector fin. The longitudinal step was 100 mm and the condenser section was 10 mm. The temperature, water heat rate, and thermal efficiency of the mathematical model results were investigated by the experimental results of the prototype for the solar water heater system under identical weather conditions.

Thermoeconomics analysis

The appropriate design for the ETSWH system, comprising the number of evacuated tubes and thermosyphon diameter, ranged from 8.49-28.58 mm and was selected based on the accumulated heat transfer of water at the storage tank as well as economic merits. The thermoeconomics method was defined by Soylemez [17]. Net saving was used for optimal thermosyphon diameter and number of evacuated tubes in the ETSWH system. The accumulated heat rate was converted to the energy cost of electric power for calculating the net saving. The net saving equation:

$$\text{Net saving} = \frac{\text{year}}{1+d} C_p H \dot{Q}_{\text{ST_tank}} - [1 - R_v(1+d)^{-\text{year}}](C_{\text{collector}}) \quad (26)$$

where C_p [Baht $k^{-1}W^{-1}h^{-1}$]* is the price of electric power, H [hrsyear $^{-1}$] – operating time for the solar water heater system, $\dot{Q}_{\text{ST_tank}}$ [Wh] – the total accumulated heat rate of solar water heater system, $C_{\text{collector}}$ [Baht] – the initial cost of the solar water heater system, d [%] – interest and R_v [%] – the resale value of the solar water heater system, and year – lifetime of solar water heater system.

For this study, the parameters were assumed for the thermoeconomics analysis. Net savings calculation was:

- the interest is 6.5 % per year [18],
- the operating time of solar water heater system is 10 years,
- the resale value of the solar system is 15% of the initial cost,
- the maintenance cost of the solar system is 10% of the initial cost, and
- the energy cost is 2.80 Baht/kWh.

* (1 Baht = 0.032\$)

These parameters were determined for optimal design of the solar water heater prototype. The prototype was constructed and tested to validate the mathematical model results with the experimental results.

Experimental set-up

The optimal design parameters for the ETSWH system were obtained from the thermoeconomics method by calculating net savings in section *Thermoeconomics analysis*. The maximum net savings for the ETSWH system was calculated from a model using a variable of thermosyphon diameter and the number of evacuated tubes. The model results showed that the optimal thermosyphon diameter and number of evacuated tubes on net saving are obtained eight evacuated tubes, 15.88 mm for the evaporator and adiabatic diameter and 22.22 mm condenser diameter. Moreover, all components constructed for the prototype of the ETSWH system were made according to appropriate parameters, which were calculated from the mathematical model presented in tab. 1.

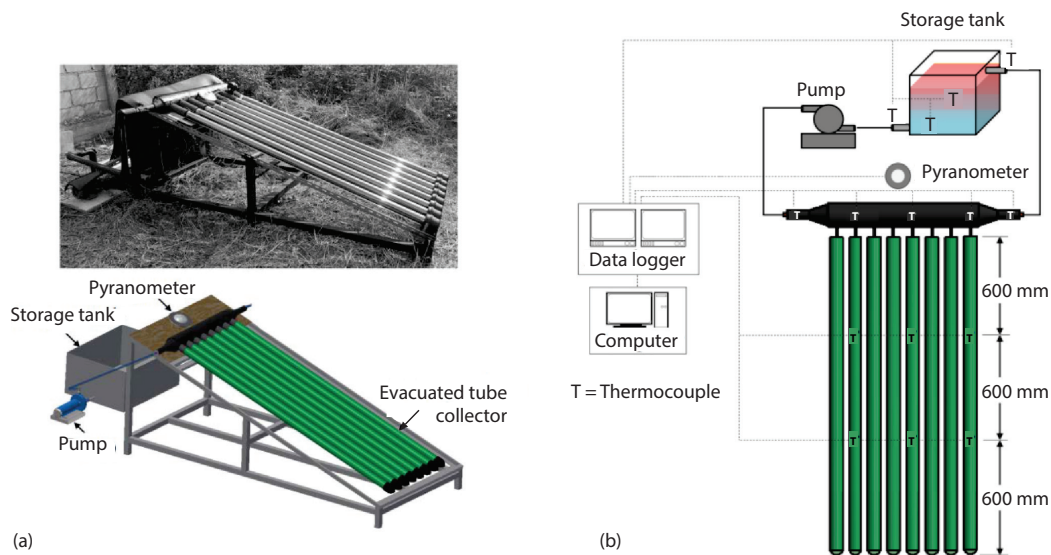


Figure 3. Experimental set-up and schematic diagram of measurement instruments for the solar water heater system; (a) experimental set-up, (b) schematic diagram of the measurement instruments

The ETSWH system was established on a stand tilted 18° facing southward, as shown in fig. 3(a). It was carried out from 8:00 a. m. to 4:00 p. m. Temperatures were measured using 38 K-type thermocouples (accuracy $\pm 1.1^\circ\text{C}$) mounted at locations shown in fig. 3(b), which were recorded using a Brainchild model VR18 data logger. Kipp and Zonen CMP3 pyranometer (accuracy $\pm 1\%$) integrated to a data logger, mounted on a surface parallel to the level of the collector. It was used to measure and record the solar intensity on the collector surface at 1 minute intervals. Wind velocity was measured and recorded using a Lutron AM-4203 anemometer (accuracy $\pm 2\%$) at the level of the solar collector every 15 minutes. The experiment was carried out from August to October 2016 in Chiang Mai province, Thailand.

Results and discussion

Effect of thermosyphon diameter and number of evacuated tube

It is widely known that solar intensity and air temperature have an effect on the system operation of solar water heaters, especially the solar intensity which should be smooth, as shown in fig. 4. With this, the solar intensity and ambient temperature on 27th February 2014 [19] in Chiang Mai province, Thailand from 9:00 a. m. to 4:00 p. m. were applied for predicting the optimal design in terms of thermosyphon diameter and the number of evacuated tubes

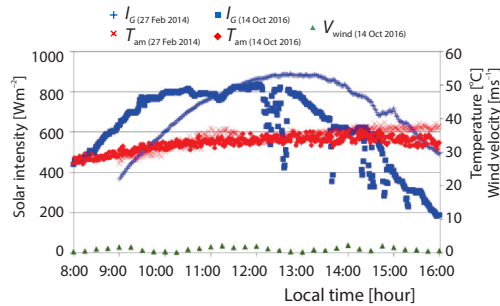


Figure 4. Variation of solar intensity and ambient temperature

for the solar water heater system. The optimal design was selected according to net savings, while net savings was calculated from the heat accumulated in water by converting to energy cost from electric price deducted by investment cost and maintenance cost of the ETSWH system. In order to analyze net savings, the number of evacuated tubes and thermosyphon diameter conditions were considered at temperatures over 65 °C due to the need for protection from Legionella and other bacterial growth harmful to personal hygiene [20].

Thermosyphon diameters and number of evacuated tubes on net savings for the solar water heater system are shown in fig. 5, in which the x-axis represents the number of evacuated tubes and the y-axis represents net savings. It can be seen that net savings from the energy price of the solar water heater system increased when increasing the thermosyphon diameter. These

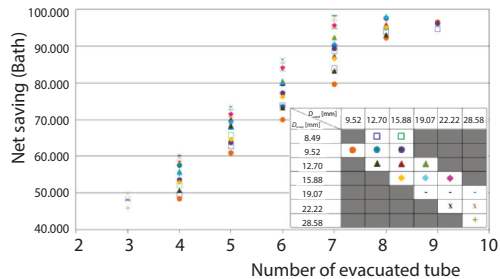


Figure 5. The effect of thermosyphon diameters and number of evacuated tube on net saving

In addition, it should be noted that the model can predict the optimal design parameters of eight evacuated tubes, as shown in fig. 5. Moreover, the optimal design parameters of the thermosyphon diameter were 15.88 mm for evaporator diameter and 22.22 mm for condenser diameter. Using these parameters, the solar water heater system obtained the maximum net savings of 98078 Baht (1 Baht = 0.032\$).

Validation of the mathematical model

To investigate the accuracy of the ETSWH model, the experimental results gained from August to October 2016 in Chiang Mai province, Thailand were selected for validation with the mathematical model results. Solar radiation, ambient temperature, and wind velocity for the experiment on 14th October 2016, as shown in fig. 4, were selected and applied to the

results were shown according to Kim and Seo [10]. Meanwhile, the effect of the number of evacuated tubes and net savings was increased by increasing the number of evacuated tubes until the number was equal to eight evacuated tubes, resulting in maximum net savings. On the other hand, the number of evacuated tubes increased over 8 caused the results of net savings to decrease slightly due to the ability of accumulating thermal energy of water being limited and heat loss being increased, according to Nada *et al.* [11].

mathematical model due to smooth solar intensity. The temperature of each component in the experiment was averaged for validation with the mathematical model results. The validation results showing the average temperature of evacuated tube, thermosyphon, and water are presented in figs. 6-8. Moreover, water heat rate and thermal efficiency of the ETSWH system were calculated and are presented in figs. 9 and 10.

The average temperature of the outer and inner evacuated tube is shown in fig. 6. It was found that the outer and inner evacuated tube temperature for the model results was in a similar trend. The results also showed good agreement with the experimental results. For the inner evacuated tube temperatures in the experiment, the temperatures were measured at the outer collector fin because the thermocouples cannot be mounted on the inner surface at other positions of the evacuated tube in a longitudinal direction. Thus, inner evacuated tube temperatures of the experiment were gained from the temperature of the collector fin as the interface between the inner evacuated was adjacent to the collector fin surface. From the results, it was found that the inner evacuated tube temperature from the model temperature was lower than the experiment after 2:30 p. m. This was because the inner evacuated tube temperature of the model was calculated from the solar intensity. Furthermore, the surrounding surface of the experiment accumulated heat from the solar intensity at noon. After that, the solar intensity decreased, meaning heat accumulated in the local surrounding surface was exothermic and would affect the heat loss of the experiment decreasing after 2:30 p. m. However, standard deviation between the experiment and model was 9.20%.

The average of thermosyphon temperatures along the local time is shown in fig. 7. It shows that the evaporator and condenser temperatures of the model were in a similar trend with the experimental results. From the evaporator temperature results, it can be seen that the model temperature was higher than the experiment from 9:30 a. m. to 2:00 p. m. because the model had negligible heat loss of the adiabatic section, which will cause heat loss to be lower than the experimental results. The average evaporator temperatures of the experimental result and the model result were 96.49 °C and 98.85 °C, respectively. For the condenser temperature, it can be seen that the experiment and model were slightly increased until the local time reached 2:30 p. m. Thereafter, these temperatures were slightly decreased until the final time. The experimental result and the model result exhibited a similar trend, with STD being $\pm 7.90\%$.

The hot water temperature of solar water heater system is presented in fig. 8. In the early morning from 8:00 a. m. to 9:00 a. m., the hot water temperature remained nearly constant for both the experiment and model due to low radiation intensity. Thereafter, the solar radiation intensity increased and the hot water temperatures for both the experiment and the model gradu-

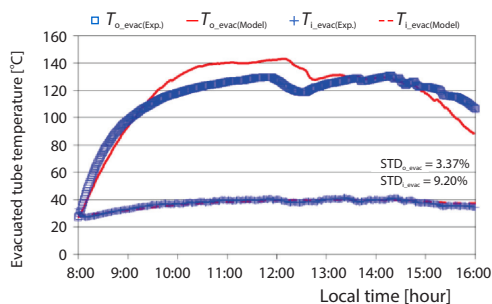


Figure 6. Temperature variation of the evacuated tube collector along the local time

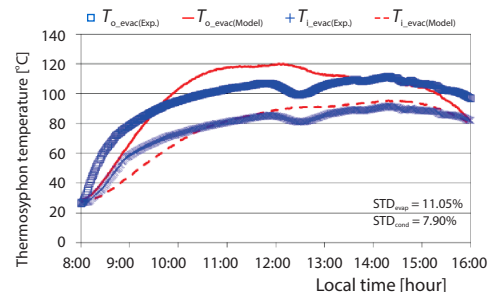


Figure 7. Variation of average thermosyphon temperature along the local time

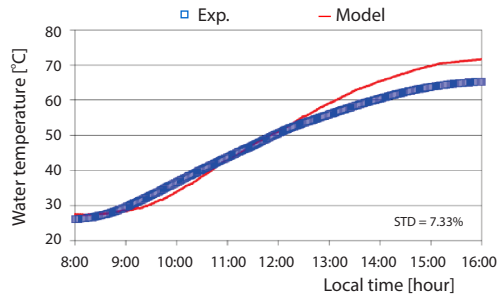


Figure 8. Variation of hot water storage tank temperature along the local time

for the solar water heater system occurred in the early evening period from about 3:30 p. m. until 4:00 p. m. at 65.25 °C and 71.66 °C of the experimental result and model result, respectively.

In order to analyze the thermal efficiency and water heat rate of the ETSWH system, calculating the average of hot water temperature every 30 minutes can be carried out. The rate of accumulated heat for water at the storage tank and thermal efficiency are presented in fig. 9. It was found that the heat rate of water was proportional to the solar energy incident on the solar water heater system. Both results showed a similar trend in the afternoon. In fig. 9 during 8:00 a. m. to 10:00 a. m., the water heat rate of the experimental result was higher than the model result because the temperature difference of water in the storage tank for the experiment was higher than the water in the storage tank for the model. The maximum heating rate of water in the experimental result occurred at 10:30 a. m. was 1050.62 W and the model result occurred at 11:00 a. m. was 1109.86 W. Besides, uncertainty analysis was based on the method explained by the Holman method, in which total uncertainty value was $\pm 5.50\%$ for water heat rate.

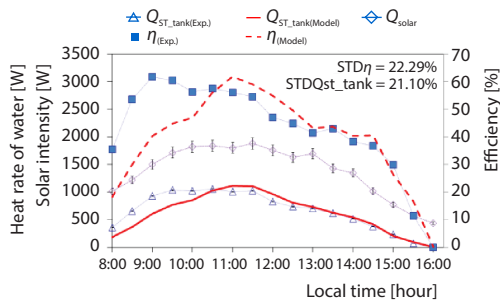


Figure 9. Variation of water heat rate and thermal efficiency along the local time

ally increased until the time reached 3:30 p. m. and then remained nearly constant till the final times. From the model results, it can be seen that the water temperature was higher than the experimental result from 12:00 p. m. to 4:00 p. m. since the model showed negligible heat loss in the water pipe between the manifold and storage tank. Moreover, heat loss in the experiment was higher after the hot water temperature was increased in the afternoon. The model was in good agreement with the experimental results. The maximum hot water temperatures

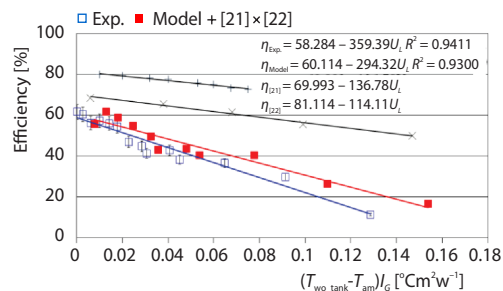


Figure 10. Relationship of $(T_{wo_tank} - T_{am})/I_G$ and thermal efficiency

For the general form of the solar water heater system, overall heat transfer coefficient and thermal efficiency of the solar water heater system is presented in fig. 10. The relationship between $(T_{wo_tank} - T_{am})/I_G$ refers to the overall heat transfer coefficient of the system. The results of regression analysis show that the equation for experiment efficiency and model efficiency was a linear function. The thermal efficiency of the experiment and model was shown to have a similar trend with the previous results [21, 22]. The slopes of the graph represent heat losses from the solar water heater system. In this study, the heat loss of the model results and experimental results were higher than with [21] and [22]. For the relationship of $(T_{wo_tank} - T_{am})/I_G$ was equal value, the thermal efficiency of the model and the experimental results were lower than the previous results [21, 22] due to heat loss in the experiment and the model being higher than

in previous results. However, the thermal efficiency of model showed good agreement with the experimental results. The experimental efficiency of the ETSWH system was 58.28%, which was about 3.04% lower than that of the model result at 60.11%. Furthermore, uncertainty analysis of $\pm 5.85\%$ for thermal efficiency and standard deviation for thermal efficiency between the experimental result and the model was 22.29%.

Conclusions

According to the experimental and mathematical model investigation of the ETSWH system, it can be concluded that.

- The thermal efficiency of the ETSWH system using the explicit finite difference method results exhibited a similar trend with the experimental results. The results of regression analysis showed that the thermal efficiency of the experimental result and the mathematical model result was 58.24% and 60.11%, respectively. To improve the accuracy of the mathematical model, heat loss for the adiabatic section of the thermosyphon and heat loss of the pipe between the manifold and storage tank are considered. However, the research results showed that the thermal efficiency of the experimental result and the mathematical model result have a similar trend and are in good agreement with previous research.
- The effects of thermosyphon diameters and the number of evacuated tubes on the net savings of the solar water heater system showed that the optimal number of evacuated tube collector and thermosyphon diameter occurred with eight evacuated tubes, 15.88 mm evaporator diameter and 22.22 mm condenser diameter. However, these parameters comprise the optimal design for climatic data in Chiang Mai province, Thailand.
- Maximum hot water temperature occurred at the final time for both the experimental result and mathematical model result at 65.25 °C and 71.66 °C, respectively.

Nomenclature

A – surface area, [m²]
 c_p – specific heat capacity, [Jkg⁻¹K⁻¹]
 I_G – solar intensity, [Wm⁻²]
 k – thermal conductivity, [Wm⁻¹K⁻¹]
 M – water mass, [kg]
 \dot{m} – mass-flow rate, [kgs⁻¹]
 Nu – Nusselt number
 \dot{Q} – heat rate, [W]
 T – temperature, [°C]
 Δt – time interval, [s]
 Z – thermal resistance, [KW⁻¹]

Greek letters

α – thermal diffusivity, [m²]
 ε – emissivity of glass
 η – thermal efficiency
 θ – dire
 τ – transmittance of ETC

Subscript

am – ambient air
 cond – condenser
 evac – evacuated glass tube
 evap – evaporator
 fin – collector fin
 i – inner/inlet
 iar – inside annular ring
 loss – heat loss
 m – manifold
 o – outer/outlet
 oar – outside annular ring
 r – r-direction/another annular ring
 ST – energy storage
 tank – storage tank
 w – water

References

- [1] Han, J, *et al.*, Solar Water Heaters in China: A New Day Dawning, *Energy Policy*, 38 (2010), 1, pp. 383-391
- [2] Liang, R., *et al.*, Performance Analysis of a New-Design Filled-Type Solar Collector with Double U-tubes, *Energy and Buildings*, 57 (2013), Feb., pp. 220-226

- [3] Morrison, G. L., et al., Water-in-Glass Evacuated Tube Solar Water Heaters, *Solar Energy*, 76 (2004), 1-3, pp. 135-140.
- [4] Budihardjo, I., Morrison, G. L., Performance of Water-in-Glass Evacuated Tube Solar Water Heaters, *Solar Energy*, 83 (2008), 1, pp. 49-56
- [5] Chow, T. T., et al., Performance Evaluation of Evacuated Tube Solar Domestic Hot Water Systems in Hong Kong, *Energy and Buildings*, 43 (2011), 12, pp. 3467-3474
- [6] Riahi, A., Taherian, H., Experimental Investigation on the Performance of Thermosyphon Solar Water Heater in the South Caspian Sea, *Thermal Science*, 15 (2011), 2, pp. 447-456
- [7] Jafarkazemi, F., et al., Energy and Exergy Efficiency of Heat Pipe Evacuated Tube Solar Collectors, *Thermal Science*, 20 (2016), 1, pp. 327-335
- [8] Samuel, L. A., Colle, S., An Experimental Study of Two-Phase Closed Thermosyphons for Compact Solar Domestic Hot-Water Systems, *Solar Energy*, 76 (2004), 1-3, pp. 141-145
- [9] Esen, M., Esen, H., Experimental Investigation of a Two-Phase Closed Thermosyphon Solar Water Heater, *Solar Energy*, 79 (2006), 5, pp. 459-468
- [10] Kim, Y., Seo, T., Thermal Performances Comparisons of the Glass Evacuated Tube Solar Collectors with Shapes of Absorber Tube, *Renewable Energy*, 32 (2007), 5, pp. 772-795
- [11] Nada, S. A., et al., Performance of a Two-Phase Closed Thermosyphonsolar Collector with a Shell and Tube Heat Exchanger, *Applied Thermal Engineering*, 24 (2004), 13, pp. 1959-1968
- [12] Azad, E., Theoretical and Experimental Investigation of Heat Pipe Solar Collector, *Experimental Thermal and Fluid Science*, 32 (2008), 8, pp. 1666-1672
- [13] Ayompe, L. M., et al., Validated TRNSYS Model for Forced Circulation Solar Water Heating Systems with Flat Plate and Heat Pipe Evacuated Tube Collectors, *Applied Thermal Engineering*, 31 (2011), 8-9, pp. 1536-1542
- [14] John, D., Anderson, J. R., *Computational Fluid Dynamics*, McGraw-Hill, New York, USA, 1995
- [15] Cengel, Y. A., *Heat Transfer a Practical Approach*, McGraw-Hill, New York, USA, 2004
- [16] ***, The ESDU, Performance of Two-Phase Closed Thermosyphon, *Engineering Sciences Data Unit*, London, 1981
- [17] Soylemez, M. S., On the Thermoeconomical Optimization of Heat Pipe Heat Exchanger HPHE for Waste Heat Recovery, *Energy Conversion and Management*, 44 (2003), 15, pp. 2509-2517
- [18] ***, Government Savings Bank, <http://www.gsb.or.th>, 2016
- [19] Wannagosit, C., et al., Computational Study of Water Heater System with Evacuated Glass Tube Solar Collector, *Proceedings*, 8th STISWB, Yangon, Myanmar, 2016, pp. 450-460
- [20] ***, The AS1056.1, Standards Australia, Storage Water Heaters – General Requirements, 1991
- [21] Caglar, A., Yamal, C., Performance Analysis of a Solar-Assisted Heat Pump with an Evacuated Tubular Collector for Domestic Heating, *Energy and Buildings*, 54 (2012), Nov., pp. 22-28
- [22] Wang, J., et al., Medium-Temperature Solar Collectors with All-Glass Solar Evacuated Tubes, *Energy Procedia*, 70 (2015), May, pp. 126-129